

Spectral function of transverse spin fluctuations in an antiferromagnet

Avinash Singh

Department of Physics, Indian Institute of Technology, Kanpur-208016, India

The spectral function of transverse spin fluctuations, including the contributions from both the single-particle and the collective (magnon) excitations in an antiferromagnet, is evaluated for the Hubbard model with NN and NNN hoppings in the full U -range from weak coupling to strong coupling. For the NN hopping model, the magnon excitations are dominant for $U > 2.5$ ($d = 2$), so that an effective spin description of the AF state holds down to a surprisingly low U value. In the weak coupling limit the spectral function is suppressed at low energies, as if due to an effective gap. NNN hopping t' leads to magnon softening and also a significant increase in the low-energy spectral function due to single-particle excitations. Evolution of the magnon spectrum with t' is studied in the strong coupling limit, and the quantum spin-fluctuation correction to sublattice magnetization in $d = 2$ and the Néel temperature in $d = 3$ are also evaluated.

75.10.Jm, 75.10.Lp, 75.30.Ds, 75.10.Hk

I. INTRODUCTION

The antiferromagnetic state of the half-filled Hubbard model with nearest-neighbour (NN) hopping is characterized by an energy gap, and the spectrum of transverse spin fluctuations consists of the low-lying, collective (magnon) excitations, as well as the single-particle excitations across the gap. Generally, there is a clear distinction between these two excitations which are well separated in energy. However, recent extensions, e.g. with disorder, [1] impurities, [2] and next-nearest-neighbour (NNN) hopping, [3] clearly show the existence of essentially gapless antiferromagnetism, arising from a variety of mechanisms. Thus, with increasing disorder (on-site potential disorder) the two Hubbard bands progressively broaden, until the band gap vanishes when the disorder strength $W \approx U$. With low- U impurities on the other hand, the effective charge gap becomes negligible due to nearly localized states on the impurities. [2] And lastly, when NNN hopping is included, a band asymmetry is introduced which reduces the band gap in the AF state, and in weak coupling there exists a region of gapless AF phase in the magnetic phase diagram. [3]

This gaplessness implies that the collective magnon excitations are no longer well defined, and actually merge with the single-particle excitations, thereby necessitating a unified scheme for the evaluation of transverse spin fluctuation. While the magnon contribution to the transverse spin fluctuations was evaluated recently, and the sublattice magnetization and the Néel temperature were obtained within a renormalized spin fluctuation theory in the whole U/t range, [4,5] in this paper we describe an alternate scheme for evaluating the transverse spin fluctuations which allows both the collective excitations and the single-particle excitations to be studied on the same footing.

Single-particle excitations are especially significant because it is precisely this part of the transverse spin spectral function which allows for a quantitative distinction of the antiferromagnetic state within the Hubbard model

from that of an equivalent Heisenberg spin model with U -dependent, extended-range spin couplings $J_{ij}(U)$, but possessing only magnon excitations. A study of the relative strengths of the magnon and single-particle excitations, in terms of the integrated spectral weights in the whole U/t range, will therefore allow for a quantitative demarcation along the U/t axis below which single-particle excitations are the dominant contribution. Thus, while in this low- U regime the AF state is not well described in terms of an effective Heisenberg spin model possessing only magnon excitations, in the intermediate and strong coupling limits use of an effective Heisenberg model with U -dependent spin couplings $J_{ij}(U)$, [6] and generally use of a spin picture [4,5] is appropriate.

Yet another significance of the single-particle excitations is interestingly connected with the spin commutation relation $[S^+, S^-] = 2S^z$. The RPA-level ground-state expectation value $\langle [S^+, S^-] \rangle_{\text{RPA}}$, involving the difference of transverse spin correlations evaluated in the AF ground state, should be identically equal to $\langle 2S^z \rangle_{\text{HF}}$, the local magnetization at the HF level. This is deduced from the fact that both RPA and HF approximations are of the same order ($O(1)$) within the systematic inverse-degeneracy expansion scheme [7] in powers of $1/\mathcal{N}$, where \mathcal{N} is the number of orbitals per site. Therefore both RPA and HF become exact in the limit $\mathcal{N} \rightarrow \infty$, when all corrections of order $1/\mathcal{N}$ or higher vanish. The magnon contribution $\langle [S^+, S^-] \rangle_{\text{RPA}}^{\text{magnon}}$ was indeed found to be in excellent agreement with the HF magnetization $\langle 2S^z \rangle_{\text{HF}}$ in the intermediate and strong coupling limits. [4] However, a discrepancy was observed at small U which was attributed to the neglect of the single-particle excitations, which become relatively more important in the weak coupling limit. We will show here that indeed when the single-particle excitations are included this discrepancy is exactly removed.

Finally, the unified scheme for incorporating both the single particle and collective excitations in the evaluation yields the complete spectrum of transverse spin excitations in the magnetic state. Calculations with realistic

models of magnetic solids can hence be used for comparison with results of scattering studies with neutrons, which are direct experimental probes into the spectrum of magnetic excitations in solids. In this regard the necessity of more realistic models which include NNN hopping etc. has been acknowledged recently from realistic band structure studies, photoemission data and neutron-scattering measurements of high- T_c and related materials. [8–11]

II. HUBBARD MODEL WITH NEXT-NEAREST-NEIGHBOUR HOPPING

We consider the following Hamiltonian on a square lattice, with hopping terms t and t' between nearest-neighbour (NN) and next-nearest-neighbour (NNN) pairs of sites $\langle ij \rangle$ and $\langle ik \rangle$ respectively,

$$H = -t \sum_{\langle ij \rangle \sigma} a_{i\sigma}^\dagger a_{j\sigma} - t' \sum_{\langle ik \rangle \sigma} a_{i\sigma}^\dagger a_{k\sigma} + U \sum_i n_{i\uparrow} n_{i\downarrow}. \quad (1)$$

Extension to the simple cubic lattice is considered in the Appendix. In the plane-wave basis defined by $a_{i\sigma} = \sqrt{\frac{1}{N}} \sum_{\mathbf{k}} e^{i\mathbf{k} \cdot \mathbf{r}_i} a_{\mathbf{k}\sigma}$, the non-interacting part of the Hamiltonian $H_0 = \sum_{\mathbf{k}\sigma} (\epsilon_{\mathbf{k}} + \epsilon'_{\mathbf{k}}) a_{\mathbf{k}\sigma}^\dagger a_{\mathbf{k}\sigma}$, where $\epsilon_{\mathbf{k}}$ and $\epsilon'_{\mathbf{k}}$ are the two free-particle energies, corresponding to NN and NNN hopping respectively,

$$\begin{aligned} \epsilon_{\mathbf{k}} &= -2t(\cos k_x + \cos k_y) \\ \epsilon'_{\mathbf{k}} &= -4t' \cos k_x \cos k_y. \end{aligned} \quad (2)$$

For the NN model, the HF-level description of the broken-symmetry AF state, and the transverse spin fluctuations have been discussed earlier in the strong, [12] intermediate, [13,14] and weak coupling [14] limits. We briefly discuss the extension for the NNN hopping. Since the NNN hopping term connects sites in the same sublattice, in the two-sublattice basis the $\epsilon'_{\mathbf{k}}$ term appears in the diagonal matrix elements of the HF Hamiltonian

$$H_{\text{HF}}^\sigma(\mathbf{k}) = \begin{bmatrix} -\sigma\Delta + \epsilon'_{\mathbf{k}} & \epsilon_{\mathbf{k}} \\ \epsilon_{\mathbf{k}} & \sigma\Delta + \epsilon'_{\mathbf{k}} \end{bmatrix} = \epsilon'_{\mathbf{k}} \mathbf{1} + \begin{bmatrix} -\sigma\Delta & \epsilon_{\mathbf{k}} \\ \epsilon_{\mathbf{k}} & \sigma\Delta \end{bmatrix} \quad (3)$$

for spin σ . Here $2\Delta = mU$, where m is the sublattice magnetization. For the NN hopping model 2Δ is also the energy gap for single-particle excitations. Since the $\epsilon'_{\mathbf{k}}$ term appears as a unit matrix, the eigenvectors of the HF Hamiltonian remain unchanged from the NN case, [12] whereas the eigenvalues corresponding to the quasiparticle energies are modified to,

$$E_{\mathbf{k}\sigma}^{(\pm)} = \epsilon'_{\mathbf{k}} \pm \sqrt{\Delta^2 + \epsilon_{\mathbf{k}}^2}. \quad (4)$$

The two signs \pm refer to the two quasiparticle bands. The band gap is thus affected by the NNN hopping term, and

it progressively decreases as $2\Delta - 4t'$ in the weak coupling limit.

As the eigenvectors of the HF Hamiltonian are unchanged, the self-consistency condition retains its form, and therefore the sublattice magnetization is independent of t' , provided there is a nonzero band gap, with the lower band occupied and the upper band empty. We will restrict ourselves only to this regime where there is no band overlap, though the gap may vanish when the two bands are just touching. The fermionic quasiparticle amplitudes $a_{\mathbf{k}\sigma}$ and $b_{\mathbf{k}\sigma}$ for spin $\sigma = \uparrow, \downarrow$ and the two quasiparticle bands are given by

$$\begin{aligned} a_{\mathbf{k}\uparrow\ominus}^2 &= b_{\mathbf{k}\downarrow\ominus}^2 = a_{\mathbf{k}\downarrow\oplus}^2 = b_{\mathbf{k}\uparrow\oplus}^2 = \frac{1}{2} \left(1 + \frac{\Delta}{\sqrt{\Delta^2 + \epsilon_{\mathbf{k}}^2}} \right) \\ a_{\mathbf{k}\uparrow\oplus}^2 &= b_{\mathbf{k}\downarrow\oplus}^2 = a_{\mathbf{k}\downarrow\ominus}^2 = b_{\mathbf{k}\uparrow\ominus}^2 = \frac{1}{2} \left(1 - \frac{\Delta}{\sqrt{\Delta^2 + \epsilon_{\mathbf{k}}^2}} \right). \end{aligned} \quad (5)$$

These relationships follow from the spin-sublattice and particle-hole symmetry in the AF state of the half-filled system.

However, this situation changes when with increasing NNN hopping t' the two bands overlap and the band gap vanishes. This overlap indicates that the low-lying states in the upper band corresponding to double occupancy are lower in energy than the high-energy states in the lower band. This results in charge transfer and consequently partially empty and doubly occupied sites. The situation is therefore analogous to the addition of holes or electrons in the half-filled Hubbard model, with all its associated complications of spin bags, strings of upturned spins, spiral and striped phases etc. [15] Thus the simple gapless AF state of the NNN hopping model, [3] which is indeed a self-consistent HF solution, may actually be unstable due to same instabilities as the hole-doped AF. Numerical HF studies do show this instability, and will be further discussed elsewhere. [16]

III. THE TRANSVERSE SPIN SPECTRAL FUNCTION

The spectral function for transverse spin fluctuations in the AF state is obtained from the imaginary part of the corresponding time-ordered propagator of the transverse spin operators S_i^- and S_j^+ at sites i and j , $\chi^{-+}(\mathbf{q}\omega) = \int dt \sum_i e^{i\omega(t-t')} e^{-i\mathbf{q} \cdot (\mathbf{r}_i - \mathbf{r}_j)} \langle \Psi_G | T[S_i^-(t) S_j^+(t')] | \Psi_G \rangle$. In terms of the RPA expression $[\chi^{-+}(\mathbf{q}\omega)]_{\text{RPA}} = [\chi^0(\mathbf{q}\omega)] / [1 - U\chi^0(\mathbf{q}\omega)]$, where $\chi^0(\mathbf{q}\omega)$ is the zeroth-order particle-hole propagator, there are two sources of contribution to the spectral function, $A(\omega) = \sum_{\mathbf{q}} \text{Im} \text{Tr}[\chi^{-+}(\mathbf{q}\omega)]$. The contribution arising from the imaginary part of $\chi^0(\mathbf{q}\omega)$ is associated with the single-particle excitations across the gap (with $\omega > 2\Delta$ for the NN model), whereas that due to the vanishing of the

denominator $1 - U\chi^0(\mathbf{q}\omega) = 0$ is associated with the collective magnon excitations (involving $\omega < 2\Delta$ for the NN model). As mentioned earlier, this latter contribution to the integrated spectral weight $\pi^{-1} \int d\omega A(\omega)$, and therefore to the transverse spin correlations $\langle S^+ S^- \rangle_{\text{RPA}}$ and $\langle S^- S^+ \rangle_{\text{RPA}}$ was recently studied in the context of quantum correction to sublattice magnetization and the Néel temperature in the whole U/t range. [4,5]

The evaluation of the transverse spin spectral function, including contributions from both the single-particle and collective excitations, is facilitated by expressing the 2×2 complex matrix $[\chi^0(\mathbf{q}\omega)]$ in terms of its eigenvalues $\lambda_{\mathbf{q}}^n(\omega)$ and eigenvectors $|\phi_{\mathbf{q}}^n(\omega)\rangle$, and we obtain

$$\begin{aligned} A(\omega) &= \sum_{\mathbf{q}} \text{ImTr}[\chi^{-+}(\mathbf{q}\omega)] = \sum_{\mathbf{q}} \text{ImTr} \frac{[\chi^0(\mathbf{q}\omega)]}{1 - U[\chi^0(\mathbf{q}\omega)]} \\ &= \sum_{\mathbf{q}} \text{ImTr} \sum_{n=1,2} \left(\frac{\lambda_{\mathbf{q}}^n(\omega)}{1 - U\lambda_{\mathbf{q}}^n(\omega)} \right) |\phi_{\mathbf{q}}^n(\omega)\rangle \langle \phi_{\mathbf{q}}^n(\omega)| \\ &= \sum_{\mathbf{q}} \text{Im} \sum_{n=1,2} \left(\frac{\lambda_{\mathbf{q}}^n(\omega)}{1 - U\lambda_{\mathbf{q}}^n(\omega)} \right). \end{aligned} \quad (6)$$

If instead of taking the trace in Eq. (6), the two diagonal matrix elements are considered separately, then

$$\begin{aligned} [\chi^0(\mathbf{q}\omega)] &= \sum_{\mathbf{k}} \left[\begin{array}{cc} a_{\mathbf{k}\uparrow\ominus}^2 a_{\mathbf{k}-\mathbf{q}\downarrow\oplus}^2 & a_{\mathbf{k}\uparrow\ominus} b_{\mathbf{k}\uparrow\ominus} a_{\mathbf{k}-\mathbf{q}\downarrow\oplus} b_{\mathbf{k}-\mathbf{q}\downarrow\oplus} \\ a_{\mathbf{k}\uparrow\ominus} b_{\mathbf{k}\uparrow\ominus} a_{\mathbf{k}-\mathbf{q}\downarrow\oplus} b_{\mathbf{k}-\mathbf{q}\downarrow\oplus} & b_{\mathbf{k}\uparrow\ominus}^2 b_{\mathbf{k}-\mathbf{q}\downarrow\oplus}^2 \end{array} \right] \frac{1}{E_{\mathbf{k}-\mathbf{q}}^{\oplus} - E_{\mathbf{k}}^{\ominus} + \omega - i\eta} \\ &+ \sum_{\mathbf{k}} \left[\begin{array}{cc} a_{\mathbf{k}\uparrow\oplus}^2 a_{\mathbf{k}-\mathbf{q}\downarrow\ominus}^2 & a_{\mathbf{k}\uparrow\oplus} b_{\mathbf{k}\uparrow\oplus} a_{\mathbf{k}-\mathbf{q}\downarrow\ominus} b_{\mathbf{k}-\mathbf{q}\downarrow\ominus} \\ a_{\mathbf{k}\uparrow\oplus} b_{\mathbf{k}\uparrow\oplus} a_{\mathbf{k}-\mathbf{q}\downarrow\ominus} b_{\mathbf{k}-\mathbf{q}\downarrow\ominus} & b_{\mathbf{k}\uparrow\oplus}^2 b_{\mathbf{k}-\mathbf{q}\downarrow\ominus}^2 \end{array} \right] \frac{1}{E_{\mathbf{k}}^{\oplus} - E_{\mathbf{k}-\mathbf{q}}^{\ominus} - \omega - i\eta}. \end{aligned} \quad (8)$$

Analytical evaluation of $[\chi^0(\mathbf{q}\omega)]$ in the strong and intermediate coupling limits has been discussed earlier for the NN hopping model, [12,13] and is described in the Appendix for the NNN hopping model. For arbitrary U , the \mathbf{k} -sum is numerically performed to evaluate the complex matrix $[\chi^0(\mathbf{q}\omega)]$, which is then diagonalized to obtain the two eigenvalues $\lambda_{\mathbf{q}}^n$ and eigenvectors $|\phi_{\mathbf{q}}^n\rangle$. The infinitesimal η is appropriately chosen according to the fineness of the \mathbf{k} and \mathbf{q} grids. Typically, the grid sizes dk and dq were taken of order 0.05 and $\eta \sim 0.01$. Summing over the whole range of \mathbf{q} values between 0 and π in each dimension then yields the spectral function $A(\omega)$ from Eq. (6), and the transverse spin correlations from Eq. (7).

The integrated spectral weight is obtained by numerically integrating the spectral function $A(\omega)$ over frequency. The collective and single-particle contributions can be evaluated separately by integrating over the ω -regions $\omega < 2\Delta$ and $\omega > 2\Delta$ respectively (for the NN case). As the single-particle excitations have a continuum distribution in Eq. (6), the evaluation of this contribution is less computationally intensive. However, for collective excitations, which are a set of delta functions, it is necessary to have in the numerical integration procedure fine enough ω - and q -grids, so that a sufficiently large number of magnon modes are picked up in the ω

we obtain the transverse spin correlations on the A(B) sublattice by integrating over frequency:

$$\begin{aligned} \langle S^+ S^- \rangle_{\text{B(A)}} &= \langle S^- S^+ \rangle_{\text{A(B)}} = \int \frac{d\omega}{\pi} \sum_{\mathbf{q}} \text{Im}[\chi^{-+}(\mathbf{q}\omega)]_{\text{A(B)}} \\ &= \int \frac{d\omega}{\pi} \sum_{\mathbf{q}} \sum_{n=1,2} \text{Im} \left(\frac{\lambda_{\mathbf{q}}^n(\omega)}{1 - U\lambda_{\mathbf{q}}^n(\omega)} \right) |\phi_{\mathbf{q}}^n(\omega)|_{\text{A(B)}}^2. \end{aligned} \quad (7)$$

Here the relationship $\langle S^+ S^- \rangle_{\text{B(A)}} = \langle S^- S^+ \rangle_{\text{A(B)}}$ between the transverse spin correlations on opposite sublattices follows from the spin-sublattice symmetry in the AF state.

IV. COMPUTATIONAL PROCEDURE AND RESULTS

To begin with the zeroth order 2×2 matrix $[\chi^0(\mathbf{q}\omega)] = i \int \frac{d\omega}{2\pi} \sum_{\mathbf{k}} [G^{\uparrow}(\mathbf{k}'\omega')] [G^{\downarrow}(\mathbf{k}' - \mathbf{q}, \omega' - \omega)]$, is evaluated in the broken-symmetry AF state. In terms of the fermionic quasiparticle amplitudes and energies, $[\chi^0(\mathbf{q}\omega)]$ is given by, [12]

$$\begin{aligned} \text{Im} \chi^0(\mathbf{q}\omega) &= \sum_{\mathbf{k}} \left[\begin{array}{cc} \frac{1}{4} & \frac{1}{4} \\ \frac{1}{4} & \frac{1}{4} \end{array} \right] \times \pi \times \\ &[\delta(E_{\mathbf{k}-\mathbf{q}}^{\oplus} - E_{\mathbf{k}}^{\ominus} + \omega) + \delta(E_{\mathbf{k}}^{\oplus} - E_{\mathbf{k}-\mathbf{q}}^{\ominus} - \omega)]. \end{aligned} \quad (9)$$

and q sums. The method described in ref. [4,5] is more efficient for evaluating the collective-excitation contribution.

Before discussing the results we first consider the two limiting cases. In the limit of vanishing interaction strength $U \rightarrow 0$, $\Delta \rightarrow 0$, we have $\chi^{-+}(\mathbf{q}\omega) = \chi^0(\mathbf{q}\omega)$, and therefore the magnon contribution vanishes. Also, as all the quasiparticle probabilities $a^2 = b^2 = 1/2$ from Eq. (5), we have from above

$$\begin{aligned} \text{Im} \chi^0(\mathbf{q}\omega) &= \sum_{\mathbf{k}} \left[\begin{array}{cc} \frac{1}{4} & \frac{1}{4} \\ \frac{1}{4} & \frac{1}{4} \end{array} \right] \times \pi \times \\ &[\delta(E_{\mathbf{k}-\mathbf{q}}^{\oplus} - E_{\mathbf{k}}^{\ominus} + \omega) + \delta(E_{\mathbf{k}}^{\oplus} - E_{\mathbf{k}-\mathbf{q}}^{\ominus} - \omega)]. \end{aligned} \quad (9)$$

In the non-interacting limit, the integrated spectral weight therefore yields

$$\lim_{U \rightarrow 0} \int \frac{d\omega}{\pi} \sum_{\mathbf{q}} \text{ImTr}[\chi^{-+}(\mathbf{q}\omega)] = 1/2. \quad (10)$$

On the other hand, in the strong coupling limit $U \rightarrow \infty$, the quasiparticle bands are narrowed to infinitesimal width, so that the imaginary part of $\chi^0(\mathbf{q}\omega)$ strengthens to delta functions at the gap frequencies $\omega = \pm U$.

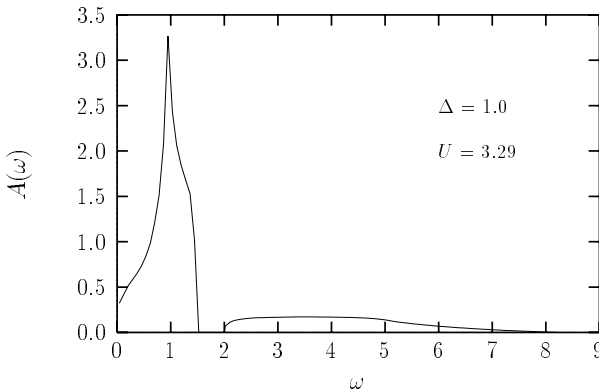


FIG. 1. The spectral function for transverse spin fluctuations obtained from Eq. (6), showing a distinct separation between the low-lying, collective excitations ($\omega < 2\Delta$) and the single-particle excitations ($\omega > 2\Delta$).

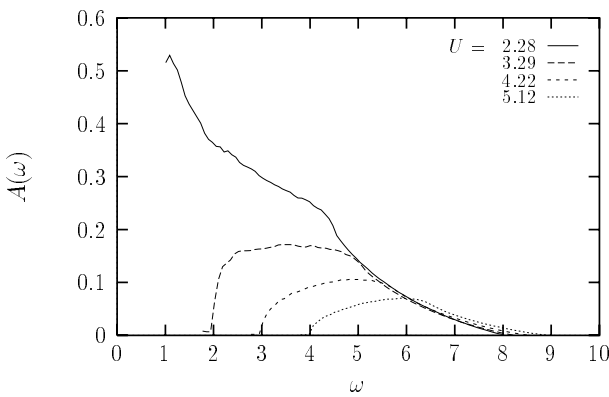


FIG. 2. The single-particle contribution to the transverse-spin spectral function $A(\omega) = \sum_q \text{Im} \text{Tr} \chi^{+}(q\omega)$, for gap values $2\Delta = 1, 2, 3, 4$, showing the rapid decrease in the spectral weight with increasing correlation.

Therefore, for both possible values of $\chi^0(\mathbf{q}\omega)$, zero or infinity, the single-particle contribution to the imaginary part of $\chi^{+}(\mathbf{q}\omega)$ vanishes. Thus, with increasing interaction strength, the spectrum of transverse spin fluctuations changes from predominantly single-particle excitations in weak coupling to predominantly magnon excitations in the strong coupling limit.

Figures 1 through 6 depict results for the NN model. Fig. 1 shows a typical transverse spin spectral function $A(\omega) = \sum_q \text{Im} \text{Tr} \chi^{+}(\mathbf{q}\omega)$, for a moderate correlation value, showing the distinct separation between the low-lying, collective excitations ($\omega < 2\Delta$) and the single-particle excitations ($\omega > 2\Delta$).

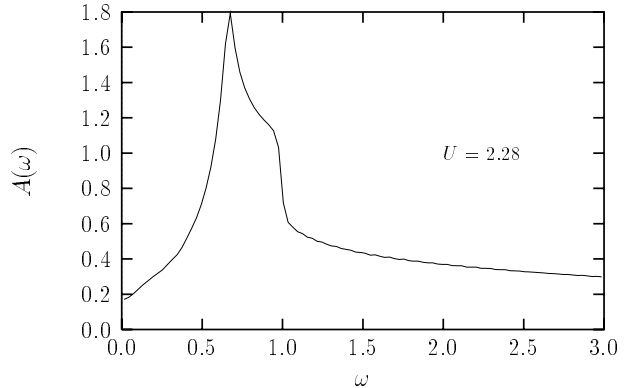


FIG. 3. The near merging of the collective ($\omega < 2\Delta$) and the single-particle ($\omega > 2\Delta$) contributions to the transverse-spin spectral function for $2\Delta = 1$.

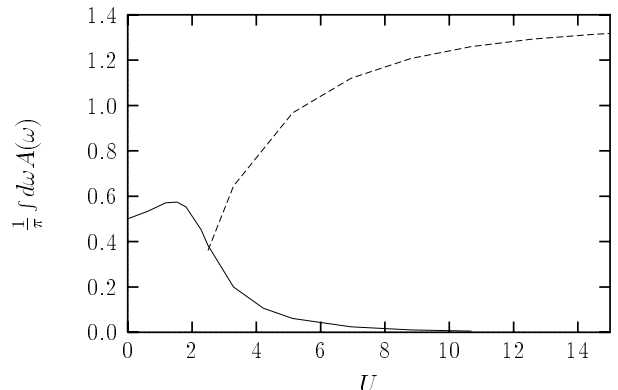


FIG. 4. The integrated spectral weights for the single-particle (solid) and collective (dashed) excitations, showing their strong suppression respectively in the strong and weak coupling limits. $U \approx 2.5$ marks the point below which an effective spin description of the antiferromagnetic state within the Hubbard model starts to fail.

Fig. 2 shows the single-particle contribution to the spectral function for moderate gap values $2\Delta = 1, 2, 3, 4$. The rapid decrease in the spectral weight with increasing correlation shows that the single-particle excitations are strongly suppressed in the strong correlation limit.

With decreasing correlation, the separation between the low-lying collective excitations and the single-particle excitations progressively decreases. Fig. 3 shows the near merging of the collective ($\omega < 2\Delta$) and the single-particle ($\omega > 2\Delta$) excitations for $2\Delta = 1$ ($U = 2.28$).

A comparison of the integrated spectral weights as a function of U is shown in Fig. 4, for the single-particle and collective excitations. While the collective excitations are seen to sharply fall-off in the weak coupling

limit,

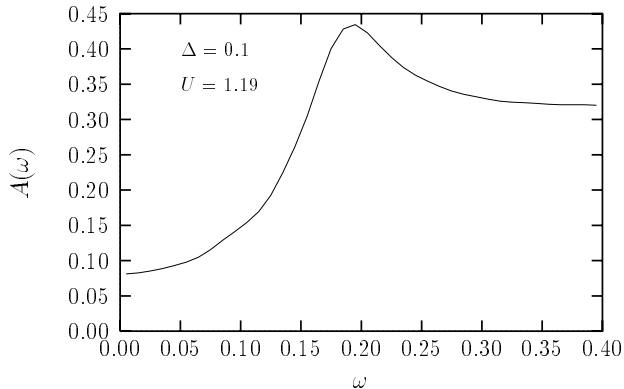


FIG. 5. The low-energy part of the transverse-spin spectral function for very low Δ , showing a gap-like suppression of excitations at low energies.

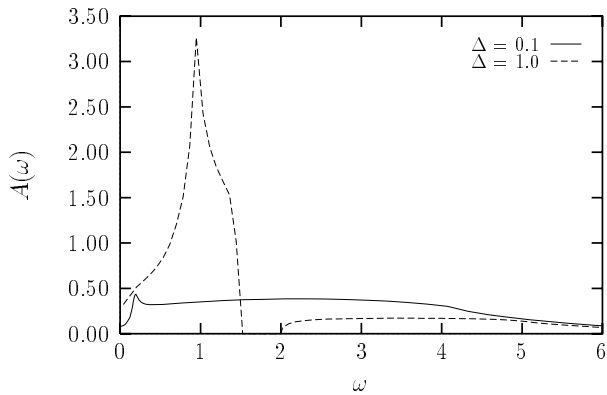


FIG. 6. The drastic suppression in the contribution of the low-energy, collective excitations in going from $U = 3.29$ ($\Delta = 1.0$) to $U = 1.19$ ($\Delta = 0.1$).

the single-particle excitations are likewise suppressed in the strong coupling limit. For $U > 2.5$, the collective (magnon) excitations are dominant, and thus an effective spin description of the antiferromagnetic state is appropriate down to a surprisingly low U value.

We now examine the role of the single-particle excitations in the sum rule following from the spin commutation relation $[S^+, S^-] = 2S^z$. As discussed in the Introduction, the RPA-level, AF ground-state expectation value $\langle [S_i^+, S_i^-] \rangle_{\text{RPA}}$, including both magnon and single-particle contributions, should be identically equal to $\langle 2S_i^z \rangle_{\text{HF}}$. The single-particle contribution to this expectation value, obtained from the transverse spin correlations $\langle S^+ S^- \rangle$ and $\langle S^- S^+ \rangle$ evaluated from Eq. (7), are shown in Table I for several U values. Also shown are the magnon contributions which were obtained earlier. [4,5] The total of the magnon and single-particle contributions is indeed in close agreement with the HF magnetization $\langle 2S_i^z \rangle_{\text{HF}}$.

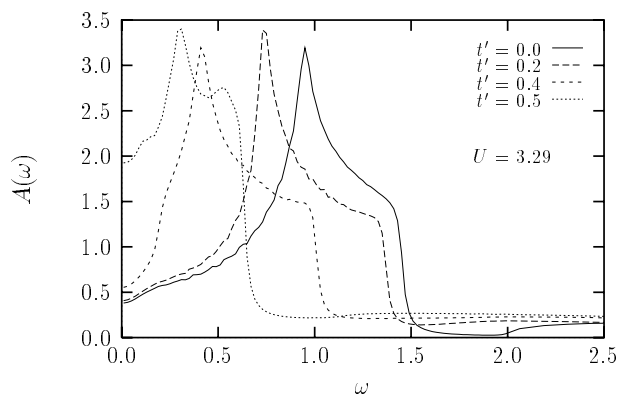


FIG. 7. Effects of the NNN hopping t' on the transverse spin spectral function, showing the shift in the magnon spectrum towards lower energy with increasing t' .

The sharp fall-off of the gapless magnon contribution in the weak coupling limit essentially leaves only the single-particle contribution. As these excitations have a minimum-energy threshold of 2Δ , the spectrum of transverse spin fluctuations essentially acquires a pseudo gap at low energies. This is clearly seen in Fig. 5, showing a gap-like suppression in the density of excitations at low energies.

Fig. 6 shows a comparison of the spectral functions for $\Delta = 0.1$ and $\Delta = 1.0$. The drastic suppression in the contribution of the low-energy, collective excitations in going from $U = 3.29$ ($\Delta = 1.0$) to $U = 1.19$ ($\Delta = 0.1$) is quite remarkable.

Fig. 7 shows the effects of the NNN hopping on the spectral function. With increasing NNN hopping t' , the magnon spectrum shifts towards lower energy, which reflects the magnon softening. There is also a substantial increase in the low-energy spectral function due to the reduction in the energy gap with NNN hopping. For $U = 3.29$, we have $\Delta = 1$, and the energy gap $2\Delta - 4t'$ just vanishes when $t' = 0.5$. It is therefore clear that the strong enhancement in the low-energy spectral function for $t' = 0.5$ is due to the gapless single-particle excitations.

TABLE I. The RPA-level expectation values of the spin commutator $[S_i^+, S_i^-]$, evaluated in the AF state from the transverse spin propagator, with contributions from the collective (magnon) excitations, and the single-particle excitations. The total is compared with the HF magnetization $\langle 2S_i^z \rangle_{\text{HF}}$.

Δ	U	$\langle [S_i^+, S_i^-] \rangle_{\text{mag}}$	$\langle [S_i^+, S_i^-] \rangle_{\text{sp}}$	$\langle [S_i^+, S_i^-] \rangle_{\text{tot}}$	$\langle 2S_i^z \rangle_{\text{HF}}$
0.6	2.499	.315	.172	.487	.480
1.0	3.292	.553	.064	.617	.607
2.0	5.127	.776	.009	.785	.781
3.0	6.948	.865			.863

This magnon softening has been analytically studied in the strong coupling limit, and the results are given in the Appendix. Due to a frustration induced by the NNN hopping term, the long-wavelength magnon-mode energy is suppressed, and for the simple cubic lattice it vanishes at $t' = 1/2$. At and above this critical value the Néel temperature T_N vanishes, indicating that the Néel state is unstable. The new phase which is stabilized beyond this point is a F-AF phase, involving antiferromagnetic ordering of spins in planes (say parallel to the x-y plane), and ferromagnetic alignment of spins along the z direction. [16] Hence $t' = 1/2$ marks the phase boundary between the AF phase with ordering wavevector $\mathbf{Q} = (\pi, \pi, \pi)$ and the F-AF phase with $\mathbf{Q} = (\pi, \pi, 0)$.

For large but finite U , there is a relative stiffening of the magnon modes due to the 3rd neighbour ferromagnetic coupling induced by the NNN hopping. This reflects a reduction in the degree of frustration, so that a slightly higher t' value is required to suppress the magnon velocity to zero. From a study of the U -dependence of this critical t' value, the magnetic phase diagram of the three dimensional Hubbard model with NNN hopping has been obtained recently. [16]

V. CONCLUSIONS

In conclusion, we have studied the spectral function of transverse spin fluctuations in an antiferromagnet using a unified approach which includes the contributions from both single-particle excitations and collective magnon excitations. For the NN hopping model in two dimensions, the integrated spectral weight was studied in the whole U range, and the collective magnon contribution was found to be dominant for $U > 2.5$, so that an effective spin description of the AF state is appropriate down to a surprisingly low U value. In the weak coupling limit the sharp fall-off of the gapless magnon contribution essentially leaves only the single-particle contribution having a minimum-energy threshold of 2Δ , so that the spectrum of transverse spin fluctuations effectively acquires a gap at low energies. The evolution of the spectral function with increasing NNN hopping, which reduces the energy gap, shows a shift of the spectral function towards lower energy due to magnon softening, and also a significant rise at low energy due to single-particle excitations.

APPENDIX

Hubbard model with NNN hopping — strong coupling limit

In this section we describe for completeness the AF properties of the half-filled Hubbard model with NNN hopping in the strong coupling limit. NNN hopping introduces a frustration in the system through the competing NNN AF interaction which enhances spin fluctuations and destabilizes the Néel state. Focussing on the enhancement of transverse spin fluctuations at the RPA level by NNN hopping, we examine the spectrum of the collective (magnon) excitations, and their contribution to the quantum spin-fluctuation correction δm_{SF} to the sublattice magnetization in two dimensions, and the reduction in the Néel temperature T_N in three dimensions.

As discussed earlier, the quasiparticle amplitudes $a_{\mathbf{k}\sigma(\pm)}$ and $b_{\mathbf{k}\sigma(\pm)}$ which form the eigenvectors of the HF Hamiltonian remain unchanged by the NNN hopping t' , provided the charge gap is finite, which is very much so in the strong coupling limit. Therefore the only change in $\chi^0(\mathbf{q}\omega)$ arises from the change in the quasiparticle energy expression given in Eq. (4), which appear in the energy denominators in Eq. (8), and we obtain, for the AA matrix element, for example

$$[\chi^0(\mathbf{q}\omega)]_{\text{AA}} = \sum_{\mathbf{k}} \frac{a_{\mathbf{k}\uparrow\oplus}^2 a_{\mathbf{k}-\mathbf{q}\downarrow\oplus}^2}{\sqrt{\Delta^2 + \epsilon_{\mathbf{k}}^2} + \sqrt{\Delta^2 + \epsilon_{\mathbf{k}-\mathbf{q}}^2} + (\epsilon'_{\mathbf{k}-\mathbf{q}} - \epsilon'_{\mathbf{k}}) + \omega} + \sum_{\mathbf{k}} \frac{a_{\mathbf{k}\uparrow\oplus}^2 a_{\mathbf{k}-\mathbf{q}\downarrow\ominus}^2}{\sqrt{\Delta^2 + \epsilon_{\mathbf{k}}^2} + \sqrt{\Delta^2 + \epsilon_{\mathbf{k}-\mathbf{q}}^2} + (\epsilon'_{\mathbf{k}} - \epsilon'_{\mathbf{k}-\mathbf{q}}) - \omega}. \quad (11)$$

Substituting $a_{\mathbf{k}\uparrow\oplus}^2 = a_{\mathbf{k}\downarrow\oplus}^2 \approx 1 - \epsilon_{\mathbf{k}}^2/4\Delta^2$ and $a_{\mathbf{k}\uparrow\oplus}^2 = a_{\mathbf{k}\downarrow\ominus}^2 \approx \epsilon_{\mathbf{k}}^2/4\Delta^2$ in the strong coupling limit, expanding the denominator in powers of t/Δ , t'/Δ , ω/Δ , and systematically retaining terms only up to order t^2/Δ^2 and t'^2/Δ^2 , we obtain after performing the \mathbf{k} -sums in two dimensions for a square lattice with $\sum_{\mathbf{k}} \epsilon_{\mathbf{k}}^2 = 4t^2$, $\sum_{\mathbf{k}} \epsilon_{\mathbf{k}}'^2 = 4t'^2$, $\sum_{\mathbf{k}} \epsilon'_{\mathbf{k}} \epsilon'_{\mathbf{k}-\mathbf{q}} = 4t'^2 \cos q_x \cos q_y$,

$$[\chi^0(\mathbf{q}\omega)]_{\text{AA}} = \frac{1}{2\Delta} \left[1 - \frac{4t^2}{\Delta^2} + \frac{2t'^2}{\Delta^2} (1 - \cos q_x \cos q_y) - \frac{\omega}{2\Delta} \right] = \frac{1}{U} \left[1 - \frac{2t^2}{\Delta^2} \left(1 + \frac{\omega}{2J} \right) + \frac{2t'^2}{\Delta^2} (1 - \cos q_x \cos q_y) \right], \quad (12)$$

where $2\Delta = mU \approx (1 - 2t^2/\Delta^2)U$ and $J = 4t^2/U$. Similarly evaluating the other matrix elements, [12], we obtain

$$[1 - U\chi^0(\mathbf{q}\omega)] = \frac{2t^2}{\Delta^2} \begin{bmatrix} 1 - \frac{J'}{J}(1 - \gamma'_{\mathbf{q}}) + \frac{\omega}{2J} & \gamma_{\mathbf{q}} \\ \gamma_{\mathbf{q}} & 1 - \frac{J'}{J}(1 - \gamma'_{\mathbf{q}}) - \frac{\omega}{2J} \end{bmatrix}, \quad (13)$$

where $\gamma_{\mathbf{q}} = (\cos q_x + \cos q_y)/2$ and $\gamma'_{\mathbf{q}} = \cos q_x \cos q_y$. Here $J = 4t^2/U$ and $J' = 4t'^2/U$ are the NN and NNN spin couplings in the equivalent Heisenberg model, and the NNN term $J'(1 - \gamma'_{\mathbf{q}})$ directly leads to a softening of the magnon mode energies. Substituting in the RPA expression, we finally obtain for the transverse spin propagator

$$[\chi^{-+}(\mathbf{q}\omega)] = -\frac{1}{2} \left(\frac{2J}{\omega_{\mathbf{q}}} \right) \begin{bmatrix} 1 - \frac{J'}{J}(1 - \gamma'_{\mathbf{q}}) - \frac{\omega}{2J} & -\gamma_{\mathbf{q}} \\ -\gamma_{\mathbf{q}} & 1 - \frac{J'}{J}(1 - \gamma'_{\mathbf{q}}) + \frac{\omega}{2J} \end{bmatrix} \cdot \left(\frac{1}{\omega - \omega_{\mathbf{q}} + i\eta} - \frac{1}{\omega + \omega_{\mathbf{q}} - i\eta} \right), \quad (14)$$

where the magnon-mode energy $\omega_{\mathbf{q}}$ is given by

$$\left(\frac{\omega_{\mathbf{q}}}{2J} \right)^2 = \left\{ 1 - \frac{J'}{J}(1 - \gamma'_{\mathbf{q}}) \right\}^2 - \gamma_{\mathbf{q}}^2. \quad (15)$$

In the long wavelength limit ($q \rightarrow 0$), with $\gamma'_{\mathbf{q}} = \cos q_x \cos q_y \approx (1 - q_x^2/2)(1 - q_y^2/2) = 1 - q^2/2$, and $\gamma_{\mathbf{q}} = (\cos q_x + \cos q_y)/2 \approx 1 - q^2/4$, the magnon energy

reduces to:

$$\omega_{\mathbf{q}} = \sqrt{2}Jq \left(1 - \frac{2J'}{J} \right)^{1/2} \quad (16)$$

showing the strong softening of low-energy modes by the NNN hopping. The spin-wave velocity vanishes in the limit $J'/J \rightarrow 1/2$. The magnon density of states

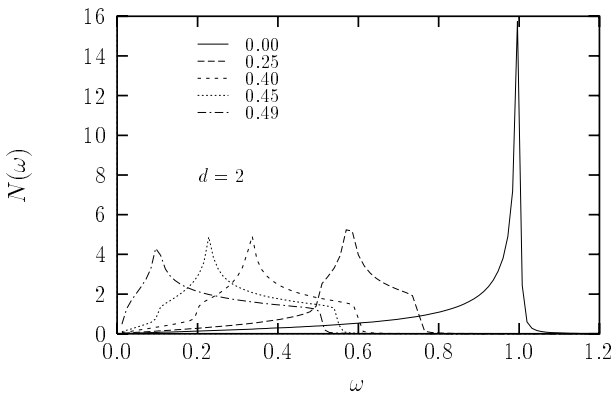


FIG. 8. The magnon density of states for different values of the ratio J'/J .

evaluated from Eq. (15) is shown in Fig. 8 for different values of the ratio J'/J . NNN hopping clearly softens the magnon energies, and transfers the magnon spectral weight from the high-energy to the low-energy region.

The strong softening of the magnon-mode energies suggests an enhancement in the transverse spin fluctuations. To examine this we evaluate the transverse spin correlations as described earlier. [4,5] From Eq. (14) for the transverse spin propagator, after performing the frequency integral we obtain the local transverse spin correlations

$$\langle S^+S^- + S^-S^+ \rangle_{\text{RPA}} = \sum_{\mathbf{q}} \frac{2J}{\omega_{\mathbf{q}}} \left\{ 1 - \frac{J'}{J} (1 - \gamma'_{\mathbf{q}}) \right\}. \quad (17)$$

The spin-fluctuation correction to sublattice magnetization is then obtained from [4,5]

$$\delta m_{\text{SF}} = \frac{\langle S^+S^- + S^-S^+ \rangle_{\text{RPA}}}{\langle S^+S^- - S^-S^+ \rangle_{\text{RPA}}} - 1 \quad (18)$$

where the denominator $\langle S^+S^- - S^-S^+ \rangle_{\text{RPA}}$ is precisely 1 for the $S = 1/2$ system due to the commutation relation $[S^+, S^-] = 2S^z$. [4,5] The spin-fluctuation correction to sublattice magnetization, evaluated from Eqs. (17), (18) is shown in Fig. 9, showing the rapid rise in transverse spin fluctuations with the frustrating NNN spin coupling J' .

$$[\chi^{-+}(\mathbf{q}\omega)] = -\frac{1}{2} \left(\frac{3J}{\omega_{\mathbf{q}}} \right) \begin{bmatrix} 1 - \frac{2J'}{J} (1 - \gamma'_{\mathbf{q}}) - \frac{\omega}{3J} & -\gamma_{\mathbf{q}} \\ -\gamma_{\mathbf{q}} & 1 - \frac{2J'}{J} (1 - \gamma'_{\mathbf{q}}) + \frac{\omega}{3J} \end{bmatrix} \cdot \left(\frac{1}{\omega - \omega_{\mathbf{q}} + i\eta} - \frac{1}{\omega + \omega_{\mathbf{q}} - i\eta} \right), \quad (20)$$

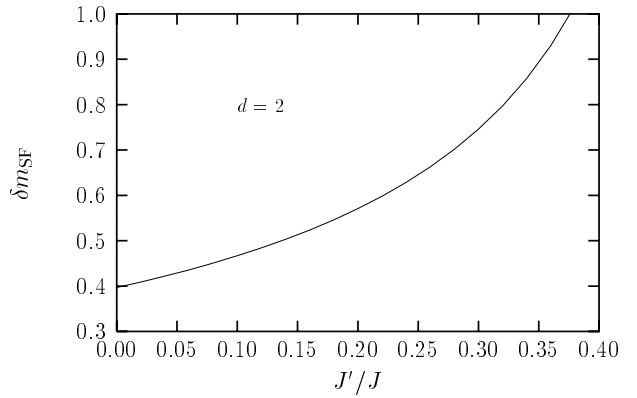


FIG. 9. The rapid increase in the spin-fluctuation correction to sublattice magnetization with the frustrating NNN spin coupling J' .

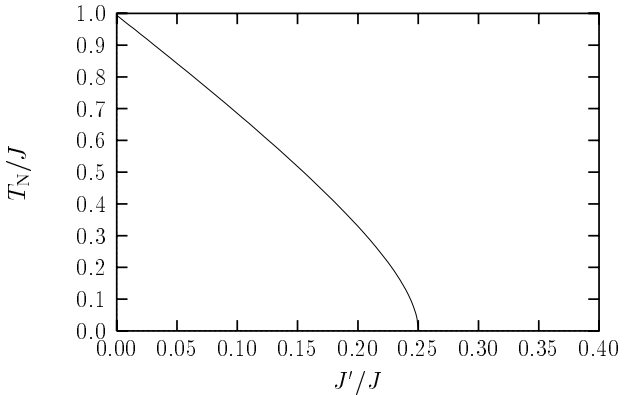


FIG. 10. The rapid decrease in the Néel temperature for the simple cubic lattice with the frustrating NNN spin coupling J' . $T_N/J = 0.989$ for $J' = 0$.

We now consider the reduction in the Néel temperature in three dimensions due to the frustrating NNN spin coupling. For this purpose we consider the NNN hopping model on a simple cubic lattice. In this case the lattice free-particle energies are

$$\begin{aligned} \epsilon_{\mathbf{k}} &= -2t(\cos k_x + \cos k_y + \cos k_z), \\ \epsilon'_{\mathbf{k}} &= -4t'(\cos k_x \cos k_y + \cos k_y \cos k_z + \cos k_z \cos k_x), \end{aligned} \quad (19)$$

and simple extension of the earlier treatment for the two-dimensional case leads to the following result for the transverse spin propagator at the RPA level

where $\gamma_{\mathbf{q}} = (\cos q_x + \cos q_y + \cos q_z)/3$ and $\gamma'_{\mathbf{q}} = (\cos q_x \cos q_y + \cos q_y \cos q_z + \cos q_z \cos q_x)/3$. The magnon-mode energy $\omega_{\mathbf{q}}$ is given by

$$\omega_{\mathbf{q}} = 3J \left[\left\{ 1 - \frac{2J'}{J} (1 - \gamma'_{\mathbf{q}}) \right\}^2 - \gamma_{\mathbf{q}}^2 \right]^{1/2}. \quad (21)$$

For small q , with $\gamma'_{\mathbf{q}} \approx 1 - q^2/3$ and $\gamma_{\mathbf{q}} \approx 1 - q^2/6$, the magnon energy reduces to

$$\omega_{\mathbf{q}} = \sqrt{3}Jq \left(1 - \frac{4J'}{J} \right)^{1/2} \quad (22)$$

which vanishes in the limit $J'/J \rightarrow 1/4$ due to the frustration effect of the NNN coupling J' . The softening of the low-energy magnon spectrum has a bearing on the Néel temperature, as discussed below.

Within the renormalized spin-fluctuation theory, [5] the Néel temperature T_N is obtained from the isotropy condition $\langle S^+ S^- + S^- S^+ \rangle_{T=T_N} = \frac{2}{3}S(S+1)$. For the NN coupling model ($J' = 0$), the Néel temperature was obtained earlier as $T_N = zJ \frac{S(S+1)}{3} f_{\text{SF}}^{-1}$ for the general case of spin S and z nearest neighbors on a hypercubic lattice. [5] For the simple cubic lattice the spin-fluctuation factor $f_{\text{SF}} \equiv \sum_{\mathbf{q}} 1/(1 - \gamma_{\mathbf{q}}^2) = 1.517$, and for $S = 1/2$ this reduces to $T_N/J = 0.989$. Extending this analysis to the present case, from the expression for the magnon propagator in Eq. (20) we obtain

$$T_N = \frac{3J}{2} \left[\sum_{\mathbf{q}} \frac{1 - \frac{2J'}{J} (1 - \gamma'_{\mathbf{q}})}{\left\{ 1 - \frac{2J'}{J} (1 - \gamma'_{\mathbf{q}}) \right\}^2 - \gamma_{\mathbf{q}}^2} \right]^{-1} \quad (23)$$

The Néel temperature, evaluated from the above equation, is shown in Fig. 10 as a function of J' . The rapid reduction of T_N with J' and the vanishing at $J' = J/4$ is due to the enhancement of transverse spin fluctuations arising from the frustration-induced softening of the long-wavelength, low-energy magnon modes. The instability at $J' = J/4$ is towards a F-AF phase with ordering

wavevector $\mathbf{Q} = (\pi, \pi, 0)$, involving antiferromagnetic ordering of spins in planes (say parallel to the x-y plane), and ferromagnetic alignment along the z direction. [16]

¹ A. Singh, M. Ulmke, and D. Vollhardt, Phys. Rev. B **58**, 8683 (1998).
² P. J. H. Denteneer, M. Ulmke, R. T. Scalettar, and G. T. Zimanyi, Physica A **251**, 162 (1998); M. Ulmke, P. J. H. Denteneer, R. T. Scalettar, and G. T. Zimanyi, Report No. cond-mat/9707068.
³ W. Hofstetter and D. Vollhardt, Ann. Phys. (Leipzig) **7**, 48 (1998).
⁴ A. Singh, Euro. Phys. Jour. B **11**, 5 (1999).
⁵ A. Singh, Report No. cond-mat/9802047.
⁶ M. A. Tusch, Y. H. Szczech, and D. E. Logan, Phys. Rev. B **53**, 5505 (1996).
⁷ A. Singh, Phys. Rev. B **43**, 3617 (1991).
⁸ P. Bénard, L. Chen, and A. -M. S. Tremblay, Phys. Rev. B **47**, 589 (1993); A. Veilleux, A. Daré, L. Chen, Y. M. Vilk, and A. -M. S. Tremblay, Phys. Rev. B **52**, 16255 (1995).
⁹ T. Tohyama and S. Maekawa, Phys. Rev. B **49**, 3596 (1993).
¹⁰ G. Stemmann, C. Pépin, and M. Lavagna, Phys. Rev. B **50**, 4075 (1994).
¹¹ O. K. Andersen, A. I. Liechtenstein, O. Jepsen, and F. Paulsen, J. Phys. Chem. Solids **56**, 1573 (1995).
¹² A. Singh and Z. Tešanović, Phys. Rev. B **41**, 614 (1990); Phys. Rev. B **41**, 11 457 (1990).
¹³ A. Singh, Phys. Rev. B **48**, 6668 (1993).
¹⁴ P. Sen and A. Singh, Phys. Rev. B **48**, 15792 (1993).
¹⁵ A. P. Kampf, Phys. Rep. **249**, 219 (1994); W. Brenig, Phys. Rep. **251**, 153 (1995).
¹⁶ A. Singh, (to be published).